Published in final edited form as:
Science. 2008 October 3; 322(5898): 110–115. doi:10.1126/science.1158111.

Ceramide Biogenesis Is Required for Radiation-Induced Apoptosis in the Germ Line of *C. elegans*

Xinzhu Deng[1], **Xianglei Yin**[1], **Richard Allan**[1], **Diane D. Lu**[1], **Carine W. Maurer**[2], **Adriana Haimovitz-Friedman**[3], **Zvi Fuks**[3], **Shai Shaham**[2], and **Richard Kolesnick**[1,*]

1*Laboratory of Signal Transduction, Memorial Sloan-Kettering Cancer Center (MSKCC), New York, NY 10021, USA*

2*Laboratory of Developmental Genetics, Rockefeller University, New York, NY, 10021, USA*

3*Department of Radiation Oncology, Memorial Sloan-Kettering Cancer Center, New York, NY 10021, USA*

Abstract

Ceramide engagement in apoptotic pathways has been a topic of controversy. To address this controversy, we tested *loss-of-function (lf)* mutants of conserved genes of sphingolipid metabolism in *Caenorhabditis elegans*. Although somatic (developmental) apoptosis was unaffected, ionizing radiation–induced apoptosis of germ cells was obliterated upon inactivation of ceramide synthase and restored upon microinjection of long-chain natural ceramide. Radiation-induced increase in the concentration of ceramide localized to mitochondria and was required for BH3-domain protein EGL-1–mediated displacement of CED-4 (an APAF-1–like protein) from the CED-9 (a Bcl-2 family member)/CED-4 complex, an obligate step in activation of the CED-3 caspase. These studies define CEP-1 (the worm homolog of the tumor suppressor p53)–mediated accumulation of EGL-1 and ceramide synthase–mediated generation of ceramide through parallel pathways that integrate at mitochondrial membranes to regulate stress-induced apoptosis.

Although studies that use genetic deficiency in ceramide production support it as essential for apoptosis in diverse models (1), many have questioned whether ceramide functions as a bona fide transducer of apoptotic signals (2). One reason for skepticism is that, despite delineation of a number of ceramide-activated proteins, no single protein has been identified as mediator of ceramide-induced apoptosis. Recent studies have suggested an alternate mode of ceramide action, based on its capacity to self-associate and locally rearrange membrane bilayers into ceramide-rich macrodomains (1 to 5 μm in diameter), which are sites of protein concentration and oligomerization (3). Ceramide may thus mediate apoptosis through its ability to reconfigure membranes, coordinating protein complexation at critical junctures of signaling cascades.

To establish the role of ceramide definitively, we used a model of radiation-induced apoptosis in *Caenorhabditis elegans* germ cells (4). Germline stem cells, located at the distal gonad tip, divide incessantly throughout adult life, with daughter cells arresting in meiotic prophase. Upon exiting prophase, germ cells become sensitive to radiation-induced apoptosis, detected morphologically just proximal to the bend of the gonadal arm (5). This apoptotic pathway is antagonized by the ABL-1 tyrosine kinase, requiring sequentially the cell cycle checkpoint genes *rad-5*, *hus-1*, and *mrt-2*; the *C. elegans* p53 homolog *cep-1*; and the genes making up the conserved apoptotic machinery, the caspase *ced-3*, the apoptotic protease activating factor

*To whom correspondence should be addressed. E-mail: r-kolesnick@ski.mskcc.org.

Supporting Online Material www.sciencemag.org/cgi/content/full/322/5898/110/DC1

1–like protein *ced-4*, the Bcl-2 protein *ced-9*, and the BH3-domain protein *egl-1*. This pathway differs from apoptotic somatic cell death, which is not subject to upstream checkpoint regulation via the CEP-1 pathway (5,6).

We identified conserved genes that regulate *C. elegans* sphingolipid intermediary metabolism and tested deletion alleles (Table 1 and table S1). Screening for mutants resistant to radiation-induced germ cell apoptosis revealed apoptosis suppression in only deletion mutants of *hyl-1* and *lagr-1*, two of the three ceramide synthase (CS) genes (Fig. 1A). CS gene products regulate de novo ceramide biosynthesis, acylating sphinganine to form dihydroceramide that is subsequently converted to ceramide by a desaturase (7). CSs contain six to seven putative transmembrane domains and a Lag1p motif [which confers enzyme activity (8)], regions conserved in the *C. elegans* orthologs. The deleted CS sequences in *hyl-1(ok976)* and *lagr-1 (gk327)* result in frameshifts that disrupt the Lag1p motifs (fig. S1A). We detected a ~1.6-kb *hyl-1* transcript in wild-type (WT) worms and a smaller ~1.35-kb transcript in *hyl-1(ok976)*, whereas we observed a ~1.4-kb *lagr-1* transcript in WT worms and a ~1.25-kb transcript in *lagr-1(gk327)* (fig. S1B). In contrast, a deletion mutant of the third *C. elegans* CS (9,10), *hyl-2 (ok1766)*, lacking a 1626-base pair fragment of the *hyl-2* gene locus that eliminates exons 2 to 5 corresponding to 74% of the coding sequence, displayed no defect in germ cell death (fig. S1C).

In N2 WTstrain young adults, apoptotic germ cells gradually increased in abundance with age from a baseline of 0.7 ± 0.1 to 1.8 ± 0.2 corpses per distal gonad arm over 48 hours. Exposure to a 120-gray (Gy) ionizing radiation dose increased germ cell apoptosis to 5.2 ± 0.3 cells 36 to 48 hours after treatment. In contrast, in *hyl-1 (ok976)* and *lagr-1(gk327)* animals, age-dependent and radiation-induced germ cell apoptosis were nearly abolished (Fig. 1A). Similar effects were observed in the *lagr-1(gk327);hyl-1(ok976)* double mutant (Fig. 1B). The rate of germ cell corpse removal was unaffected in CS mutants, excluding the possibility that defective corpse engulfment elevated corpse numbers (table S2). In contrast, *loss-of-function (lf)* mutations of *hyl-1* or *lagr-1* did not affect developmental somatic cell death, nor did the *lf hyl-2 (ok1766)* mutation (table S3). These studies indicate a requirement for two *C. elegans* CS genes for radiation-induced germline apoptosis.

To confirm ceramide as critical for germline apoptosis, we injected C_{16}-ceramide into gonads of young adult WT worms. C_{16}-ceramide is the predominant ceramide species in apoptosis induction by diverse stresses in multiple organisms (11) and in low abundance in *C. elegans* (12,13). C_{16}-ceramide microinjection resulted in time- and dose-dependent increases in germ cell apoptosis (Fig. 1C), with a median effective dose of ~0.05 μM gonadal ceramide. Peak effect occurred at ~0.1 μM gonadal ceramide at 36 hours (6.6 ± 0.8 versus 1.5 ± 0.4 cell corpses per distal gonad arm, $P < 0.0001$), qualitatively and quantitatively mimicking the 120-Gy effect in WT worms. In contrast, C_{16}-dihydroceramide, which differs from C_{16}-ceramide in a trans double bond at sphingoid base position four to five, was without effect (0.71 ± 0.28 cell corpses per distal gonad arm at ~1 μM), indicating specificity for ceramide in apoptosis induction. Furthermore, C_{16}-ceramide microinjection into *lagr-1(gk327);hyl-1(ok976)* animals (~1 μM gonadal ceramide) resulted in a 5.7-fold increase in germ cell apoptosis (from 0.60 ± 0.17 to 3.43 ± 0.88, $P < 0.0001$) (Fig. 1D). Note that the baseline level of apoptosis in *lagr-1 (gk327);hyl-1(ok976)* was less than one-half that in WT worms. Moreover, ~0.005 μM gonadal ceramide, a concentration without impact on germ cell apoptosis, completely restored radiation (120 Gy)–induced apoptosis, an effect inhibitable in a *lf ced-3* background (Fig. 1E). C_{16}-ceramide's ability to bypass the genetic defect and restore the radiation-response phenotype is strong evidence that *hyl-1* and *lagr-1* represent legitimate *C. elegans* CS genes. Animals with *sphk-1(ok1097)*, a null allele of sphingosine kinase (SPHK), which prevents conversion of ceramide to its anti-apoptotic derivative sphingosine 1-phosphate (S1P) (14), displayed high baseline germ cell death and were hypersensitive to radiation-induced germ cell apoptosis (fig.

S2, A and B), inhibitable (by 85 ± 9%) in a *lagr-1(gk327);sphk-1(ok1097)* double mutant. Collectively, these studies identify ceramide as a critical effector of radiation-induced germ cell apoptosis, although they do not define its mode of engaging the apoptotic pathway.

Inactivation of the *C. elegans* ABL-1 ortholog in the *lf* mutant *abl-1(ok171)* (or by RNA interference) increases baseline and post-radiation germ cell apoptosis, modeling radiation hypersensitivity phenotypes (15). To order CS action relative to ABL-1, we generated *hyl-1 (ok976);abl-1(ok171)* and *lagr-1(gk327);abl-1(ok171)* and a triple mutant lagr-1(gk327);hyl-1 (ok976);abl-1(ok171). lf hyl-1 or *lagr-1* in an *abl-1(ok171)* genetic background prevented the time-dependent increase in physiologic germ cell apoptosis and completely blocked radiation-induced apoptosis (Fig. 2A, left). Similarly, *lagr-1(gk327);hyl-1(ok976);abl-1(ok171)* displayed inhibition of baseline and radiation-induced germ cell apoptosis (Fig. 2A, right). Thus, increased germ cell apoptosis in irradiated *abl-1(ok171)* depends on the CS genes *hyl-1* and *lagr-1*.

In *C. elegans*, DNA damage activates the p53 homolog CEP-1, which is required for transcriptional up-regulation of the BH3-only proteins, EGL-1 and CED-13, that in turn activate the core apoptotic machinery (CED-9, CED-4, and CED-3) (6,16). Exposure of *hyl-1 (ok976)* and *lagr-1 (gk327)* to 120 Gy increased *egl-1* transcripts four- to fivefold at 9 hours after irradiation (Fig. 2B, left), whereas *ced-13* expression was enhanced five- to sixfold (Fig. 2B, right)—levels comparable to those detected in irradiated WTworms. Thus, the loss of CS did not affect CEP-1 activation upon irradiation, suggesting that ceramide and CEP-1 might function in parallel, coordinately conferring radiation-induced germ cell death.

We reasoned that in contrast to radiation-induced germ cell apoptosis, which apparently requires increased abundance of both BH3-only proteins and ceramide, C_{16}-ceramide provided exogenously might act independent of p53-mediated *egl-1* expression by maximizing the effect of baseline EGL-1. In fact, microinjected C_{16}-ceramide partially restored germ cell death in *cep-1(gk138)* from 0.4 ± 0.13 to 2.5 ± 0.32 corpses per distal gonad arm (Fig. 2C) ($P < 0.001$). As C_{16}-ceramide is inactive in the *lf egl-1* mutant *egl-1(n1084n3082)* (Fig. 2C), it appears that there is a requirement for at least a baseline level of BH3-only proteins for ceramide-induced apoptosis. Consistent with this notion, C_{16}-ceramide administration did not increase *egl-1* and *ced-13* transcription (1.2 ± 0.1– and 0.8 ± 0.1–fold of control, respectively, at 5 hours). Furthermore, inactivating the core apoptotic machinery in *lf ced-3(n717)* and *ced-4(n1162)* or in gain-of-function *ced-9(n1950)* animals, which abolish radiation-induced germline apoptosis, similarly abolished C_{16}-ceramide-induced death (Fig. 2C). Collectively, these data indicate that ceramide acts in conjunction with BH3-only proteins upstream of the mitochondrial commitment step of apoptosis in the *C. elegans* germ line.

As these studies point to a mitochondrial site of ceramide action, we devised an immune histochemical approach to evaluate whether ceramide might increase in the mitochondria of *C. elegans* germ cells. We took advantage of the increased frequency of germ cell apoptosis in *abl-1(ok171)*, anticipating a maximized ceramide signal upon irradiation in this strain. Gonads from unirradiated or irradiated worms were dissected, opened by freeze-cracking (17), and then stained with MID15B4, a specific anti-ceramide antibody [see the supporting online material (SOM)]. Mitochondria were localized with an antibody to the mitochondrial marker protein OxPhos Complex IV subunit I (COX-IV) or by Rhodamine B staining (18). COX-IV staining (green) before and after irradiation displayed a prominent perinuclear distribution reminiscent of mitochondrial topography in some mammalian cell systems (Fig. 3A) (19,20). Ceramide staining (red) displayed a similar profile and at baseline was faint, increasing 2.4-fold at 24 hours post-irradiation (Fig. 3A and fig. S3) ($P < 0.0001$). Merging the two signals (red and green) revealed that ceramide accumulation was distinctively mitochondrial (yellow). Radiation-induced ceramide accumulation was abrogated in *lagr1(gk327);hyl-1(ok976);abl-1*

(ok171) animals (Fig. 3A). Similarly, ceramide increase was abrogated in irradiated *lagr-1 (gk327);hyl-1(ok976)* as compared with WT animals (1.2- versus 3.9-fold of unirradiated controls, respectively). These results define ionizing radiation-induced ceramide accumulation in the *C. elegans* germ line as mitochondrial in origin, mediated via the classic ceramide biosynthetic pathway.

We examined whether mitochondrial ceramide accumulation was required for CED-4 redistribution to nuclear membranes. In nonapoptotic somatic cells, CED-4 is sequestered to mitochondria by binding CED-9. When displaced by EGL-1, CED-4 targets nuclear membranes and activates caspase CED-3, necessary for the effector phase of apoptosis (21-24). For these studies, *abl-1(ok171)* and *lagr-1(gk327);hyl-1(ok976);abl-1(ok171)* animals were exposed to 120 Gy, and germ cells were released from gonads and stained with antibodies against *C. elegans* CED-4 and Ce-lamin, a nuclear membrane marker. CED-4 and Ce-lamin colocalization by confocal microscopy (yellow merged signal) served as readout for nuclear CED-4 redistribution. After irradiation nuclear CED-4 staining intensity increased 4.3-fold from 0.59 ± 0.03 to 2.53 ± 0.42 arbitrary fluorescence units in *abl-1(ok171)* (Fig. 3, B and C) ($P < 0.001$). Consistent with reduced germ cell apoptosis (Fig. 2A), nuclear CED-4 staining is significantly reduced in *lagr-1(gk327);hyl-1(ok976);abl-1(ok171)* (Fig. 3, B and C) [$P < 0.001$ versus *abl-1(ok171)*]. Specifically, baseline CED-4 intensity at the nuclear membrane is lower in *lagr-1(gk327);hyl-1(ok976);abl-1(ok171)* than in *abl-1(ok171)*, increasing post-irradiation only to the control level of unirradiated *abl-1(ok171)* worms (Fig. 3C), an effect probably of biologic relevance as the biophysical effects of ceramide on membrane structure are concentration-dependent (1,3).

We also used *opls219* worms, a strain expressing a CED-4::GFP fusion protein (where GFP is green fluorescent protein), which permits in vivo detection of CED-4 trafficking (25). *opls219* worms were cultured on plates containing Rhodamine B to stain mitochondria (red). Merged images detect mitochondrial CED-4 as a yellow signal (red and green overlay), whereas nonmitochondrial CED-4 appears green. Although a low-intensity green CED-4 signal was detected in nuclear membranes of unirradiated germ cells, the large majority of CED-4 was present in mitochondria before irradiation. At 36 hours postradiation, the CED-4 signal was markedly reduced in mitochondria, relocalizing primarily to nuclear membranes as bright green platform-like structures (arrows in lower left panel in bottom of Fig. 3D). In eight worms, overall reduction in CED-4 mitochondrial colocalization upon irradiation was ~50% ($P < 0.0001$), abrogated in *lagr-1(gk327);opls219* (fig. S4). Consistent with the anti–CED-4 antibody staining (Fig. 3B), the loss of mitochondrial CED-4 signal in *opls219* was accompanied by a twofold increase in nuclear CED-4 signal, blocked entirely in *lagr-1 (gk327);opls219* (to 0.9 ± 0.1 fold of control). These results indicate that mitochondrial ceramide contributes substantively to CED-4 displacement from mitochondrial membranes during radiation-induced germ cell apoptosis.

Our data indicate that the ceramide synthetic pathway is required for radiation-induced apoptosis of *C. elegans* germ cells. The most parsimonious molecular ordering suggests that CS (as well as its enzymatic product ceramide) functions on a pathway that is parallel to the CEP-1/p53–EGL-1 system. The coordinated function of these two pathways occurs at the mitochondrial commitment step of the apoptotic process. We hypothesize that ceramide may recompartmentalize the mitochondrial outer membrane, yielding a permissive microenvironment for EGL-1–mediated displacement of CED-4, the trigger for the effector stage of the apoptotic process.

Supplemental Material

Refer to Web version on PubMed Central for supplementary material.

References and Notes

1. Gulbins E, Li PL. Am. J. Physiol. Regul. Integr. Comp. Physiol 2006;290:R11. [PubMed: 16352856]
2. Hofmann K, Dixit VM. Trends Biochem. Sci 1998;23:374. [PubMed: 9810222]
3. Goni FM, Alonso A. Biochim. Biophys. Acta 2006;1758:1902. [PubMed: 17070498]
4. Materials and methods are available as supporting material on *Science* Online.
5. Gartner A, Milstein S, Ahmed S, Hodgkin J, Hengartner MO. Mol. Cell 2000;5:435. [PubMed: 10882129]
6. Hofmann ER, et al. Curr. Biol 2002;12:1908. [PubMed: 12445383]
7. Geeraert L, Mannaerts GP, van Veldhoven PP. Biochem. J 1997;327:125. [PubMed: 9355743]
8. Spassieva S, et al. J. Biol. Chem 2006;281:33931. [PubMed: 16951403]
9. That *hyl-1* and *hyl-2* encode ceramide syntheses is clearly shown by their ability to restore growth to nearly WT levels when expressed in Lag1/Lac1 double yeast mutants (10).
10. Martinou, J-C.; Riezman, H. personal communication
11. Pewzner-Jung Y, Ben-Dor S, Futerman AH. J. Biol. Chem 2006;281:25001. [PubMed: 16793762]
12. A small amount of C16:0:0 ceramide with a C17 sphingosine base (2% of the amount of the most aboundant species C22:0:1) can be detected in *C. elegans* extracts (13).
13. Riezman, H. personal communication
14. Taha TA, et al. FASEB J 2006;20:482. [PubMed: 16507765]
15. Deng X, et al. Nat. Genet 2004;36:906. [PubMed: 15273685]
16. Schumacher B, et al. Cell Death Differ 2005;12:153. [PubMed: 15605074]
17. DuerrJSWorm Book2007www.wormbook.org. The *C. elegans* Research Community, WormBook
18. Labrousse AM, Zappaterra MD, Rube DA, van der Bliek AM. Mol. Cell 1999;4:815. [PubMed: 10619028]
19. De Vos K, et al. J. Biol. Chem 1998;273:9673. [PubMed: 9545301]
20. del Peso L, Gonzalez VM, Inohara N, Ellis RE, Nunez G. J. Biol. Chem 2000;275:27205. [PubMed: 10846174]
21. Conradt B, Horvitz HR. Cell 1998;93:519. [PubMed: 9604928]
22. Fairlie WD, et al. Cell Death Differ 2006;13:426. [PubMed: 16167070]
23. Chen F, et al. Science 2000;287:1485. [PubMed: 10688797]
24. Yan N, et al. Mol. Cell 2004;15:999. [PubMed: 15383288]
25. Zermati Y, et al. Mol. Cell 2007;28:624. [PubMed: 18042457]

26. We thank Caenorhabditis Genetics Center and National BioResource Project-Japan for the strains provided; H. R. Horwitz for the anti–CED-4 antibody; Y. Gruenbaum for the anti–Ce-lamin-antibody; M. O. Hengartner for the strain opls219; and S. Davidor, D. Chau, H. Lee, J. Mesicek, and the Molecular Cytology and Genomics Core Laboratory of MSKCC for the technical assistance. This work was supported by grants CA85704 (R.K.), CA105125−03 (A.H.-F.), and 2R01HD42680−06 (S.S.).

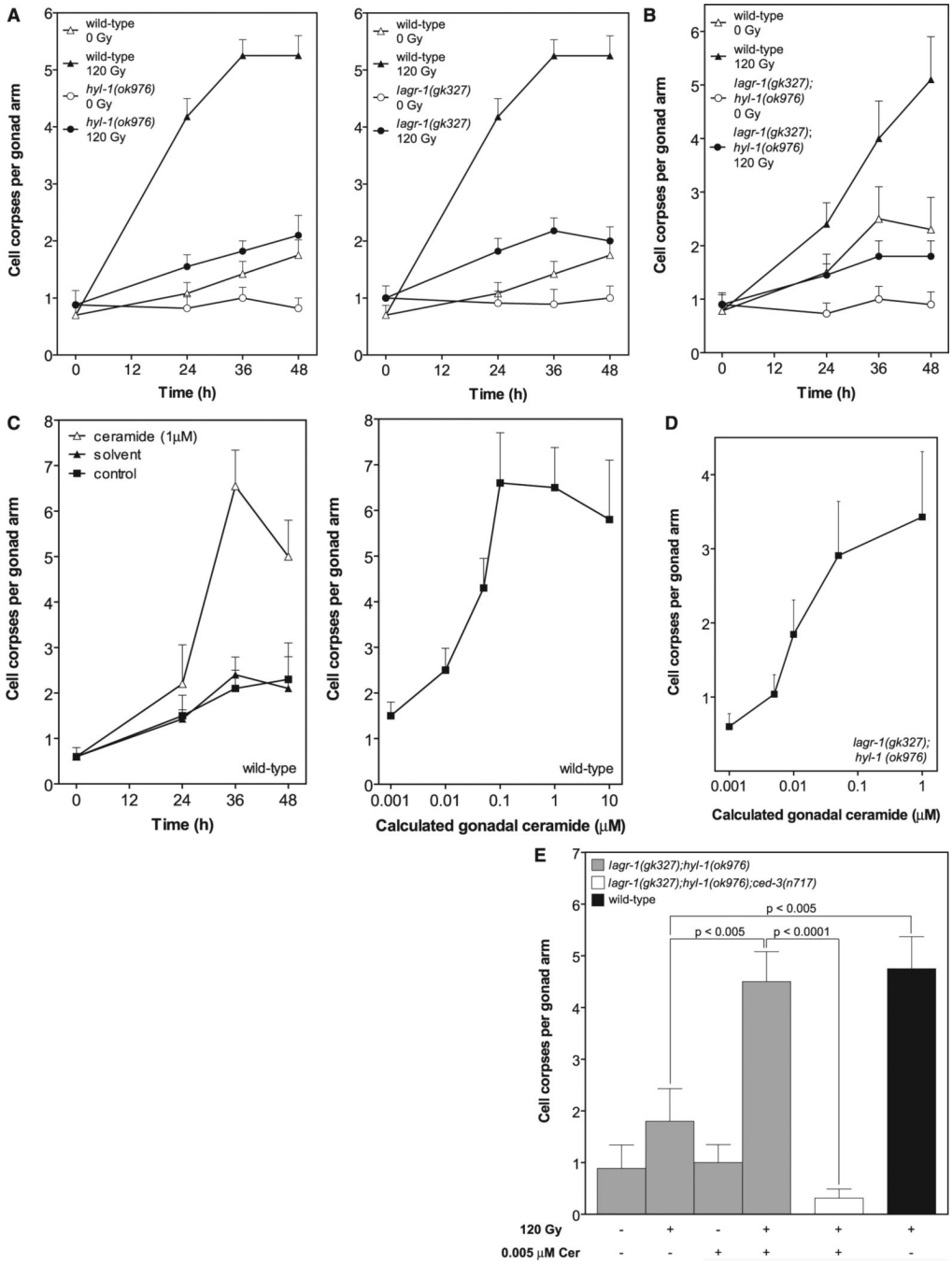

Fig. 1.

lf hyl-1 and *lagr-1* prevent radiation-induced germ cell apoptosis, reversible by C_{16}-ceramide. WT and mutant worms were synchronized at 20°C and irradiated (**A**, **B**, and **E**) or injected with C_{16}-ceramide into the posterior gonad (**C** to **E**) at 24 hours after the L4 stage. The posterior gonad distal arm was scored for cell corpses under Nomarski optics. Time dependence of germ cell corpse induction in *hyl-1(ok976)* (left) and *lagr-1(gk327)* (right) (A) and in *lagr-1 (gk327);hyl-1(ok976)* (B) after 120 Gy is shown. WT data are identical in (A), left and right; these panels were separated for clarity. C_{16}-ceramide microinjection induces time- (left) and dose-dependent (right, at 36 hours) germ cell apoptosis in WT worms (C) and dose-dependent apoptosis in *lagr-1(gk327);hyl-1(ok976)* at 36 hours (D). Gonadal ceramide concentration was

calculated as described in the SOM. (E) Sublethal C_{16}-ceramide microinjection restores radiation (120 Gy)-induced germ cell apoptosis to *lagr-1(gk327);hyl-1(ok976)*. Data (mean ± SEM, represented by error bars) are collated from ≥15 worms per group in (A) to (E).

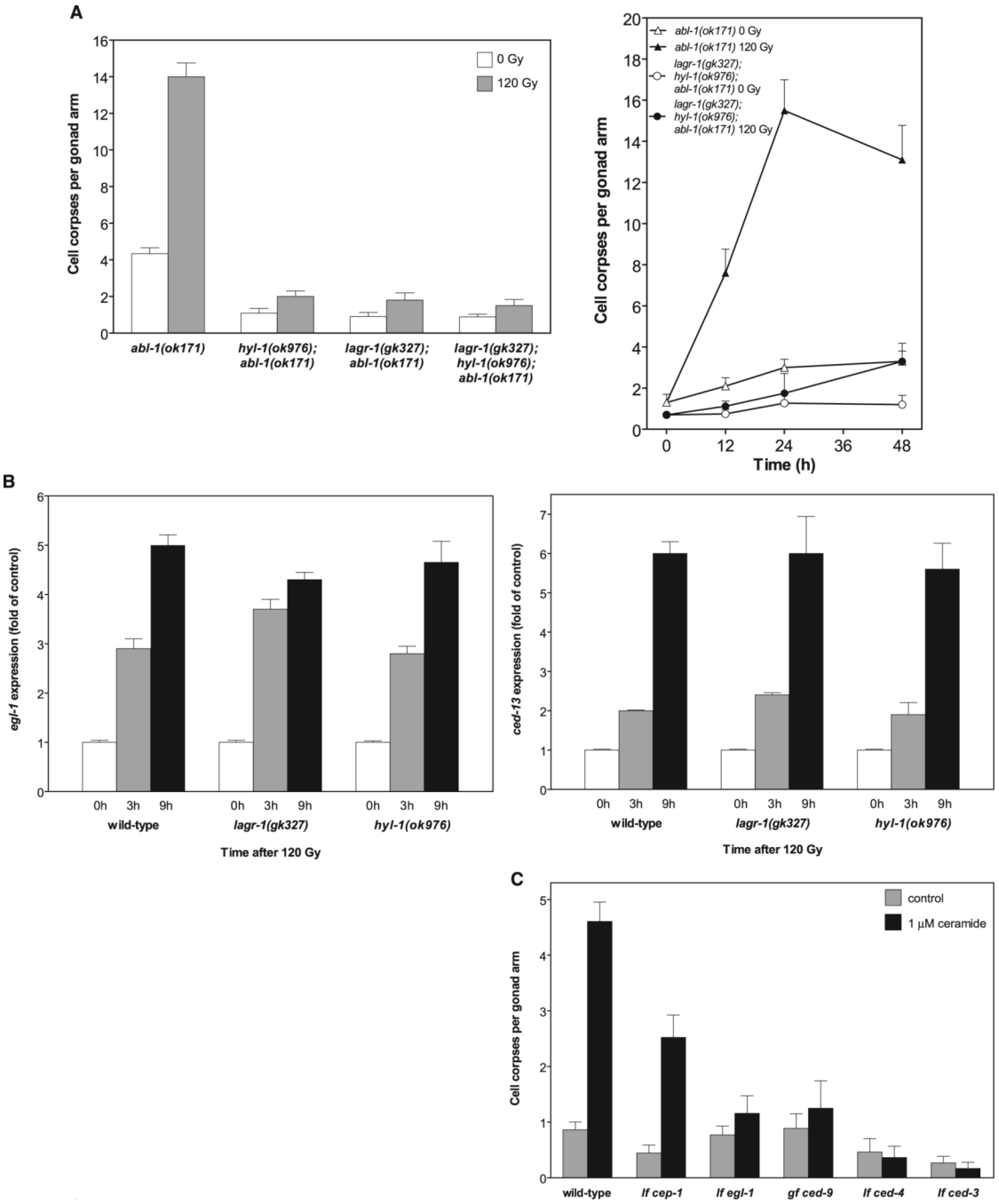

Fig. 2.

Role of ceramide in CEP-1/p53–mediated germ cell apoptosis. (**A**) *hyl-1* and *lagr-1* are epistatic to *abl-1* in germ cell apoptosis. Germ cell apoptosis was scored in abl-1(ok171), hyl-1 (ok976);abl-1(ok171), lagr-1(gk327);abl-1(ok171), and *lagr-1(gk327);hyl-1(ok976);abl-1 (ok171)* at 36 hours (left) and in *lagr-1(gk327);hyl-1(ok976);abl-1(ok171)* at the indicated times after exposure to 120 Gy (right). Data (mean ± SEM, represented by error bars) are collated from 10 to 15 worms per group. (**B**) *hyl-1* and *lagr-1* deletions do not affect 120-Gy–induced p53-mediated *egl-1* (left) and *ced-13* (right) up-regulation measured by reverse transcription polymerase chain reaction. Data (mean ± SEM) are compiled from three

experiments. (**C**) Baseline EGL-1 is required for C_{16}-ceramide (~1 μM gonadal ceramide)–induced germ cell apoptosis. Studies were performed as in Fig. 1B. Data (mean ± SEM) are collated from ≥15 worms per group.

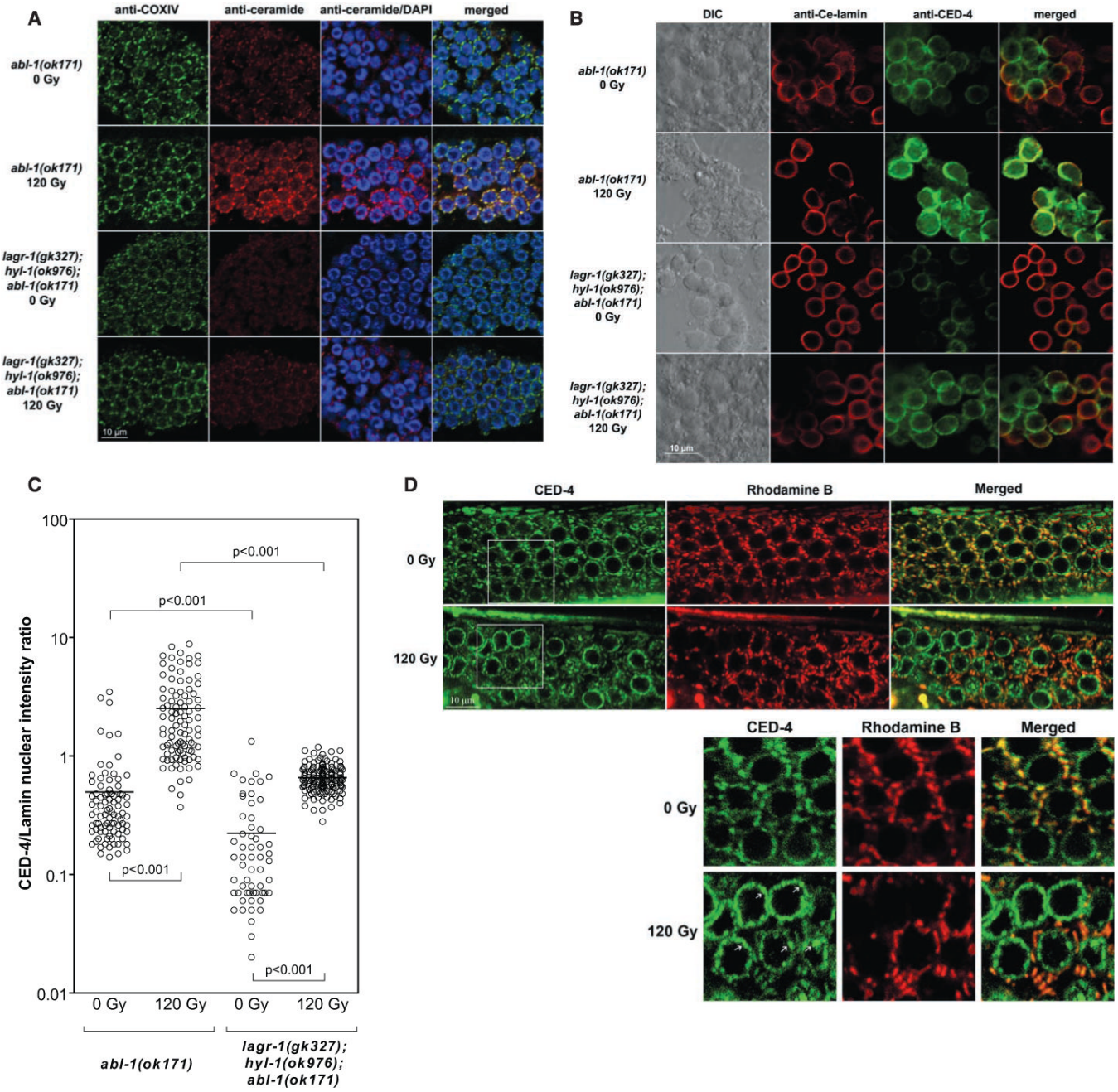

Fig. 3.

Mitochondrial ceramide mediates CED-4 displacement. (**A**) Gonads were dissected from young adult *abl-1(ok171)* and *lagr-1(gk327);hyl-1(ok976);abl-1(ok171)* at 24 hours after 120 Gy and stained with anti–COX-IV antibody (green), anti-ceramide antibody (red), and 4′,6′-diamidino-2-phenylindole (blue). (**B** and **C**) Germ cells were released from gonads of young adult *abl-1(ok171)* and *lagr-1(gk327);hyl-1(ok976);abl-1(ok171)* at 24 hours after 120 Gy and stained with anti–Ce-lamin (red) and anti–CED-4 (green). CED-4/lamin intensity in individual germ cell nuclei (circles) was measured using Metamorph software. Horizontal bars indicate means from ≥50 nuclei per group. In *lagr-1(gk327);hyl-1(ok976);abl-1(ok171)*, the baseline CED-4/lamin ratio is reduced by 63%, and the post-radiation fold and absolute change are reduced by 40% and 78%, respectively, as compared with *abl-1(ok171)* animals. (**D**) L1 larvae

of *opls219*, cultured in Rhodamine B–containing plates until the young adult stage, were exposed to 120 Gy, and GFP (CED-4) and Rhodamine B (mitochondria) signals were imaged at 36 hours post-irradiation. Images represent single confocal planes from the distal gonad of *opls219* (upper panels). Boxed insets (lower panels) were enlarged 1.75 times to ease the observation of colocalized CED-4/Rhodamine B mitochondrial yellow signal (top right bottom panel) pre-irradiation and green nuclear CED-4 platformlike structures post-irradiation (white arrows in bottom left lower panel).

Table 1

Role of *C. elegans* orthologs of sphingolipid metabolism in radiation-induced apoptosis. The family of sphingolipids and associated metabolic enzymes involved in ceramide intermediary metabolism, conserved from yeast to humans is shown on at left. Thick arrows designate the de novo ceramide synthetic pathway. Enzymes listed in bold indicate *C. elegans* enzymes for which *lf* alleles were screened for germ cell apoptosis at 36 hours post–120 Gy (shown at right). Apoptosis inhibition (+) was interpreted relative to WT-irradiated controls. Asterisks indicate hypersensitivity to radiation-induced apoptosis. At least 20 worms were counted per allele. SPT, serine palmitoyltransferase; 3-KSR, 3-ketosphinganine reductase; CerS, ceramide synthase; DES, dihydoceramide desaturase; CerK, ceramide kinase; SMase, sphingomyelinase; CDase, ceramidase; SphK, sphingosine kinase; S1PPL, S1P lyase.

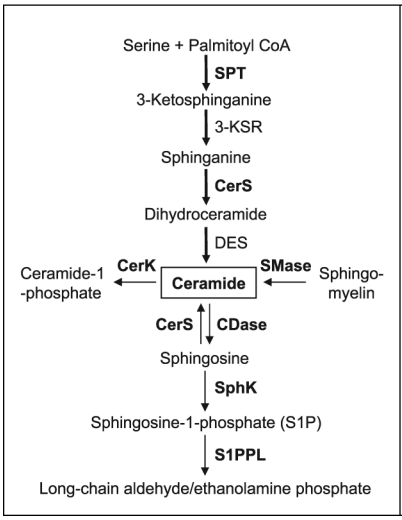

Mammalian gene product	*C. elegans* orthologous gene(s)	Sequence name	Alleles	Apoptosis inhibition
SPT 1	*sptl-1*	C23H3.4	*ok1693*	–
SPT 2	*sptl-3*	T22G5.5	*ok1927*	–
CerS	*hyl-1*	C09G4.1	*ok976*	+
	hyl-2	K02G10.6	*ok1766*	–
	lagr-1	Y6B3B.10	*gk327* *gk331*	+ +
Acid CDase		F27E5.1	*ok564*	–
SphK-1	*ok1097*	C34C6.5a,b	*ok1097*	–*
S1PPL 1	*tag-38*	B0222.4	*tm470*	–
CerK		T10B11.2	*ok1252*	–
Acid SMase	*asm-1*	B0252.2	*kk-1*	–
	asm-2	ZK455.4	*ok183*	–
	asm-3	W03G1.7a,b	*tm2384*	–
Neutral SMase		T27F6.6	*tm2178*	–